Signal Transduction

Molecular Cancer Research

The Role of Nitric Oxide Synthase Uncoupling in Tumor Progression

Christopher S. Rabender[1], Asim Alam[1], Gobalakrishnan Sundaresan[2], Robert J. Cardnell[3], Vasily A. Yakovlev[1], Nitai D. Mukhopadhyay[4], Paul Graves[5], Jamal Zweit[2], and Ross B. Mikkelsen[1]

Abstract

Here, evidence suggests that nitric oxide synthases (NOS) of tumor cells, in contrast with normal tissues, synthesize predominantly superoxide and peroxynitrite. Based on high-performance liquid chromatography analysis, the underlying mechanism for this uncoupling is a reduced tetrahydrobiopterin:dihydrobiopterin ratio (BH4:BH2) found in breast, colorectal, epidermoid, and head and neck tumors compared with normal tissues. Increasing BH4:BH2 and reconstitution of coupled NOS activity in breast cancer cells with the BH4 salvage pathway precursor, sepiapterin, causes significant shifts in downstream signaling, including increased cGMP-dependent protein kinase (PKG) activity, decreased β-catenin expression, and TCF4 promoter activity, and reduced NF-κB promoter activity. Sepiapterin inhibited breast tumor cell growth *in vitro* and *in vivo* as measured by a clonogenic assay, Ki67 staining, and 2[18F]fluoro-2-deoxy-D-glucose–deoxyglucose positron emission tomography (FDG-PET). In summary, using diverse tumor types, it is demonstrated that the BH4:BH2 ratio is lower in tumor tissues and, as a consequence, NOS activity generates more peroxynitrite and superoxide anion than nitric oxide, resulting in important tumor growth–promoting and antiapoptotic signaling properties.

Implications: The synthetic BH4, Kuvan, is used to elevate BH4:BH2 in some phenylketonuria patients and to treat diseases associated with endothelial dysfunction, suggesting a novel, testable approach for correcting an abnormality of tumor metabolism to control tumor growth. *Mol Cancer Res; 13(6); 1034–43. ©2015 AACR.*

Introduction

Interest in nitric oxide (NO) as a signaling molecule in normal and cancer cells has developed because of links between chronic inflammatory diseases, such as diabetes and reactive oxygen and reactive nitrogen species (ROS/RNS), with cancer (1). NO can have both protumorigenic and antitumorigenic activities, depending on concentration and levels of other ROS (2). For example, inhibition of endogenous NO synthases (NOS) blocks the growth of some, but not all, tumor cells by direct cytotoxic effects on the tumor cells or by inhibiting tumor endothelial cells (3, 4). In contrast, increased activity of inducible NOS (iNOS) in breast and colorectal cancer cells upregulates tumor growth, promoting Wnt/β-catenin signaling (5).

NO/RNS are essential for autocrine-regulated oncogenic Ras-driven pancreatic tumor growth (6). Akt phosphorylation and activation of endothelial NOS (eNOS) stimulates RNS-dependent oxidation or S-nitrosylation of Cys^{118} of Ras, resulting in cytoprotective signaling through Akt. Regulation of receptor Tyr kinase pathways, e.g., EGFR, can be achieved by inhibiting counteracting protein Tyr phosphatases by RNS-mediated oxidation of their active site Cys, e.g., SHP-2 (7, 8). PTEN also has an active site Cys sensitive to oxidation, and its oxidation by RNS inhibits PTEN-activating antiapoptotic Akt signaling (9). RNS activate cytoprotective NF-κB transcriptional activity by nitrating Tyr^{181} of IκBα, causing its dissociation from NF-κB (10). Simulating a chronic inflammatory environment by treating MCF10A cells with low levels of RNS donors or coculturing with activated macrophages stimulates Tyr nitration and activity of PP2A, leading to the downregulation of BRCA1 expression and reduced homologous recombination DNA repair. The latter is compensated by enhanced nonhomologous end-joining repair, potentially promoting chromosomal instability, a hallmark of tumor progression (11).

Alternatively, NO can inhibit growth-promoting pathways of tumors. For example, S-nitrosylation of the p65 subunit of NF-κB or of IKKβ blocks NF-κB transcriptional activity (12). Increasing cellular cGMP with 5′-phosphodiesterase (PDE5) inhibitors or overexpression of cGMP-dependent protein kinase G (PKG), a downstream effector of NO, inhibits colorectal and breast tumor growth (13, 14).

Given the technical difficulties of directly measuring NO in cells and tissues, most studies with tumors assume that NOS synthesize NO. However, as documented in the vasculature literature, NOS has two activities: NO or O_2^-/$ONOO^-$ synthesis (15). For all three isoforms of NOS, the catalytic cycle involves the cofactor BH4 donating electrons to the NOS Fe^{2+}–O_2 complex, initiating

[1]Department of Radiation Oncology, Virginia Commonwealth University, Richmond, Virginia. [2]Department of Radiology and Center for Molecular Imaging, Virginia Commonwealth University, Richmond, Virginia. [3]Department of Thoracic/Head and Neck Medical Oncology, The University of Texas MD Anderson, Houston, Texas. [4]Department of Biostatistics, Virginia Commonwealth University, Richmond, Virginia. [5]Department of Radiation Oncology, New York Methodist Hospital, Weill Cornell Medical College, Brooklyn, New York.

Note: Supplementary data for this article are available at Molecular Cancer Research Online (http://mcr.aacrjournals.org/).

Corresponding Author: Ross B. Mikkelsen, Virginia Commonwealth University, Box 58, Richmond, VA 23298-0058. Phone: 804-628-0857; Fax: 804-826-6042; E-mail: rmikkels@vcu.edu

doi: 10.1158/1541-7786.MCR-15-0057-T

Arg oxidation. The ratio of [BH4] to its oxidation product [BH2] is critical because both bind to the active site with equal affinity. When tissue BH4:BH2 is low, as found in patients with chronic inflammatory diseases, more O_2^-/$ONOO^-$ and less NO are generated (16). This catalytic uncoupling also occurs at very low [Arg] or with increased levels of endogenous NOS inhibitors (17, 18).

We showed that sepiapterin, a salvage pathway precursor for BH4, prophylactically blocked dextran sodium sulfate (DSS)-induced colitis in mice and significantly reduced the incidence of colorectal tumors in an azoxymethane/DSS mouse model for colorectal cancer (19). High-performance liquid chromatography (HPLC) analyses of total colon biopterins were inconclusive, although there was a trend for lower BH4:BH2 in colons from mice treated with DSS that was reversed with sepiapterin. However, colonic cGMP levels were significantly reduced in colons of mice drinking DSS, and this was reversed with sepiapterin by a mechanism sensitive to an inhibitor of the NO-activated soluble guanylate cyclase (sGC). Inhibiting sGC also blocked the protective effects of sepiapterin on colitis. Oral sepiapterin inhibited expression of inflammatory cytokines (IL1β, IL6, and IL17A), reduced infiltration of inflammatory cells (neutrophils and macrophages), and significantly inhibited the increased protein Tyr nitration in the diseased colons. These results are consistent with DSS/chronic inflammation–induced uncoupling of NOS, although we could not eliminate that BH4 or sepiapterin also protects sGC from oxidative inactivation (20).

To further explore the role of NOS uncoupling in tumor growth, we measured BH4:BH2 in diverse tumors, both *in vitro* and *in vivo*. Downstream signaling pathways relevant to breast cancer growth and sensitive to NO/RNS have been evaluated in terms of NOS coupling and tumor cell survival.

Materials and Methods

Biologic materials

Cell lines from the ATCC, authenticated through short tandem repeat profiling, were frozen as early-passage stocks after receipt from the vendor. Cells were cultured for fewer than 6 months after thawing. All cell lines were grown in 10% FCS in RPMI-1640 plus penicillin–streptomycin. Subcutaneous (s.c.) tumor xenografts were created in the hind legs of athymicNCr-nu/nu mice (3). MCF7 xenograft growth was supported by 17β-estradiol pellets (1.5 mg, 60-day release; Innovative Research of America) inserted s.c. on the backs of mice. Breeding pairs of MMTVneu mice were from The Jackson Laboratory. Drinking water was doped with 40 μg/mL sepiapterin or 0.64 mg/kg/day (19), significantly less than used in studies on vascular function (21). All animal experiments conform to protocols approved by the Institutional Animal Care and Use Committee of Virginia Commonwealth University.

Human colorectal tumor samples and paired normal tissues were provided by the Tissue and Data Acquisition and Analysis Core of Massey Cancer Center as sections from optimal cutting temperature (OCT) blocks were prepared at the time of surgery. These samples were obtained through an Institutional Review Board approved specimen anonymization agreement.

Reagents

Reagents included biopterins (Schircks Laboratories), KT5823, and the cGMP Elisa kit (Cayman Chemical Co.). Antibodies were Actin, IκBα, VASP (Santa Cruz), p65, $pSer^{157}$, and $pSer^{239}$ VASP (Cell Signaling Technology), PKG1β (Stressgen), Ki67 (NOVUS Biologicals), 3-nitrotyrosine (Life Technologies), β-catenin (BD Transduction), and fluorophore-conjugated secondary antibodies (Rockland). Expression plasmids for VASP, iNOS, eNOS, and GCH1 were from Addgene.

Cell and biochemical analyses

Clonogenic assays and analytic methods for biopterins and cGMP have been described (3, 19). OCT blocks of human colon tissue were dissolved in PBS, and the tissue was collected by centrifugation prior to extracting in 0.1 N HCl for HPLC analysis. O_2^- generation was assayed by a fluorescence HPLC assay (22). Protein S-nitrosylation was detected by the biotin switch method (7).

For T-cell factor/lymphoid enhancer factor (TCF/LEF) promoter activity, cells were treated with PKGIβ siRNA premix (Qiagen) or sepiapterin. After 24 hours, cells were transfected by lipofectamine/plus with a luciferase-tagged TCF/LEF reporter construct (Addgene) in sepiapterin-free medium. Three hours later, the medium was changed with fresh sepiapterin, and luciferase activity was measured 24 hours later. A luciferase reporter plasmid (Clontech) was used to measure NF-κB promoter activity (10).

PET/CT imaging

Fasted and anesthetized (2% isoflurane) animals were tail vein injected with 300 μCi[^{18}F]FDG (IBA Molecular). After 60 minutes of 2[18F]fluoro-2-deoxy-D-glucose (FDG) uptake, PET/CT images were acquired in the Inveon Preclinical System (Siemens Healthcare) without attenuation correction. Images were processed using the manufacturer's recommended calibration procedures, and a phantom of known volume and activity was acquired prior to the study. OSEM3D-MAP reconstructions used Inveon Acquisition Workplace 1.5 for region-of-interest (ROI) analysis in the Inveon Research Workplace 4.1. The percentage of injected dose/g of tissue (%ID/g) was calculated after decay corrections using the formula: $\%ID/g = (C_t/ID) \times 100$, where C_t is the concentration of the radiotracer in the tissue obtained from the PET images after ROI analysis.

Immunohistochemistry

Tumors frozen in liquid N_2 were embedded in OCT. Cryosections (6 μm) fixed in ice-cold acetone were blocked with goat serum prior to staining with DAPI and antibodies. Images were captured using the Ariol Digital Pathology Platform. Quantitation was obtained with ImageJ software using DAPI staining for normalization.

Statistical analysis

Except where indicated, a one-way ANOVA with the Dunnett *post hoc* test was used for statistical analysis with $P \leq 0.05$ considered statistically significant.

Results

BH4:BH2 is low in tumor cells and increases with sepiapterin supplementation

The BH4:BH2 of tumor cells measured with an HPLC assay (Supplementary Fig. S1) was significantly lower relative to that of normal tissues examined. This is true regardless of their origin (breast, head and neck, epidermoid, and colorectal) or whether grown in tissue culture, as xenografts, or in a spontaneous mouse

breast cancer model (MMTVneu). Low BH4:BH2 is also observed in human colorectal carcinoma biopsies compared with that found in paired adjacent "normal" colon tissue (Table 1; paired *t* test, $n = 4$, $P < 0.001$). That the paired "normal" biopsy sample has a relatively lower BH4:BH2 from that expected for normal tissue is possibly a consequence of the inflammatory state of tissue adjacent to tumor. Insufficient amounts of normal human breast epithelial tissue for the HPLC analysis precluded a similar analysis for breast cancer tissues.

BH4:BH2 is regulated in part by the rate-limiting enzyme for BH4 synthesis, GTP-cyclohydrolase-1 (GCH1), or by a salvage pathway in which sepiapterin is converted to BH4 through the activities of sepiapterin reductase and dihydrofolate reductase (DFHR; ref. 23). Targeting either pathway is effective in manipulating BH4:BH2. Transient transfection of MCF7 cells at about 50% efficiency with an expression plasmid for GCH1 increases BH4:BH2 approximately 6-fold (Table 1). Incubating cells with sepiapterin increased BH4:BH2 maximally at 6 hours and sustained for at least 16 hours (Supplementary Fig. S2 and Supplementary Table S1). Depending on the cell type, 20 μmol/L sepiapterin for 16 hours increases BH4:BH2 between 3- and 17-fold. For breast and squamous carcinoma xenografts and spontaneous MMTVneu mammary tumors, drinking water containing sepiapterin for 48 hours elevates tumor BH4:BH2 from 3- to 7-fold.

To establish that sepiapterin promotes an increased BH4:BH2 via the salvage pathway, additional experiments used the sepiapterin reductase inhibitor, N-acetylserotonin (NAS), and the high-affinity NOS inhibitor, Nω-nitro-L-arginine (L-NNA). Coincubation of sepiapterin and NAS substantially blocks the sepiapterin-induced increase in BH4:BH2, with no effect on basal BH4:BH2 in MCF7 or MDA-231 cells (Table 2). L-NNA modestly increases BH4:BH2 in cells not incubated with sepiapterin ($P = 0.01$, MCF7; $P = 0.03$, MDA-231). Coincubation of L-NNA with sepiapterin also increases BH4:BH2 in MCF7 cells relative to sepiapterin alone ($P = 0.002$). This was not statistically significant with MDA-231 cells ($P = 0.1$). That NOS inhibition enhances BH4:BH2 is consistent with an uncoupling mechanism whereby NOS-produced peroxynitrite directly oxidizes BH4 autopropagating NOS uncoupling (17). We also demonstrated that NADPH oxidase activity contributes to BH4 oxidation in that incubation of cells with its peptide inhibitor, gp91 ds-tat, caused significant increases in the BH4:BH2 (Table 2).

Table 1. BH4:BH2 measurements in multiple cell types *in vitro* and *in vivo*

	BH4:BH2	BH4:BH2 + sepiapterin
Normal mouse tissue[a]		
Colon	7.1 ± 0.6	n/d
Lung	11.1 ± 2.4	n/d
Liver	8.3 ± 0.8	n/d
Kidney	13.4 ± 1.2	n/d
In vitro tumor cell lines[a]		
A431	0.3 ± 0.5	2.1 ± 0.6
MCF7	0.6 ± 0.2	10.1 ± 0.4
MDA231	1.0 ± 0.1	5.8 ± 0.2
HT29	1.1 ± 0.4	2.8 ± 0.1
MCF10A	1.2 ± 0.2	3.1 ± 0.3
MCF7-GCH1[b]	3.6 ± 0.2	n/d
In vivo tumor xenografts[a]		
Fadu	0.8 ± 0.2	2.6 ± 0.3
MCF7	1.1 ± 0.1	7.9 ± 0.2
MDA231	1.4 ± 0.3	6.4 ± 0.4
Paired MMTVneu mouse tissue[a]		
Mammary fat pad	3.8 ± 0.5 ($n = 4$)	n/d
Mammary tumors	1.0 ± 0.2 ($n = 8$)	2.8 ± 0.5 ($n = 8$)
Paired human colon tissue[c]		
Normal colon	4.5 (3.5–6.1)	n/d
Human CRC	2.3 (1.5–3.5)	n/d

[a]Mean ± SEM. With *in vitro* samples, cells were harvested 16 hours after incubation with 20 μmol/L sepiapterin. With xenograft and spontaneous tumors, mice drank sepiapterin-loaded water for 2 days. For all comparisons between samples with or without sepiapterin, a $P < 0.005$ was calculated by a two-tailed Student *t* test.

[b]MCF7 cells transiently transfected with GCH1 and BH4:BH2 levels measured 48 hours later.

[c]Paired samples of human colon tumor (CRC) and adjacent normal colon from the same patients ($n = 4$) with average and range of values shown.

Table 2. BH4:BH2 measurements in MCF7 and MDA-231 cells treated with without sepiapterin, L-NNA, NAS, and a NADPH oxidase inhibitor

	MCF7 BH4:BH2	MDA-231 BH4:BH2
Control	0.5 ± 0.2	0.9 ± 0.3
+ Sepiapterin	6.1 ± 0.4	5.8 ± 0.3
+L-NNA	1.1 ± 0.1	1.6 ± 0.2
+L-NNA + sepiapterin	8.1 ± 0.3	6.4 ± 0.4
+NAS	0.5 ± 0.2	1.0 ± 0.2
+ sepiapterin +NAS	2.6 ± 0.5	2.9 ± 0.3
+gp91ds-tat	1.8 ± 0.2	2.3 ± 0.3

NOTE: Cells were incubated with 20 μmol/L sepiapterin with or without 200 nmol/L L-NNA,1 mmol/L NAS, or 5 μmol/L gp91ds-tat for 6 hours before harvesting. Mean ± SEM; $n = 3$.

Recoupling NOS activity with sepiapterin

To test whether increased BH4:BH2 enhances NO production, cellular cGMP levels were measured. As a positive control, MCF7 cells were incubated with the NO donor, S-nitrosoglutathione (GSNO). There is a progressive increase in the basal levels of cGMP with increasing sepiapterin concentration (Fig. 1A). Coincubation with L-NNA blocks the increase, indicating that sepiapterin is acting through the NO-dependent sGC. Sepiapterin also enhanced cGMP levels in MCF7 and MDA-231 tumor xenografts (Fig. 1B). Both MCF7 and MDA-231 cells express cGMP-dependent PK G-1β (24, 25). To measure its enzymatic activity, we monitored phosphorylation of Ser^{239} of the endogenous PKG substrate, VASP. Sepiapterin treatment of MCF7 cells transiently transfected with VASP enhances Ser^{239} VASP phosphorylation (Fig. 1C, top two panels). We also examined the cAMP-dependent protein kinase A (PKA) site Ser^{157}. Western blot analysis of VASP $pSer^{157}$-VASP showed no change in phosphorylation with sepiapterin, although there was a robust response to the PKA agonist forskolin (Fig. 1C, bottom two panels).

L-NNA inhibits both eNOS and iNOS with a selectivity of about 20-fold for eNOS (26). Because MCF7 and MDA-231 cells express both eNOS and iNOS isoforms, but iNOS catalytic activity is 100-fold greater than that of eNOS, we tested whether a highly selective inhibitor for iNOS, 1400W (5,000-fold selectivity), also blocked sepiapterin-increased cGMP levels (27, 28). As shown in Supplementary Fig. S3, 1400W effectively blocked sepiapterin-induced cGMP levels. That the catalytic activity of iNOS is 100-fold greater than eNOS argues that iNOS is the dominant, but depending on physiologic conditions perhaps not the only, NOS isoform stimulating sGC. Regardless of the isoform, exogenous sepiapterin increases BH4:BH2, thereby recoupling NOS and stimulating sGC.

Uncoupled NOS produces O_2^- and increasing cellular BH4 reduces cell production of O_2^- (15). To functionally assess NOS recoupling, O_2^- was measured using a HPLC-fluorescence assay

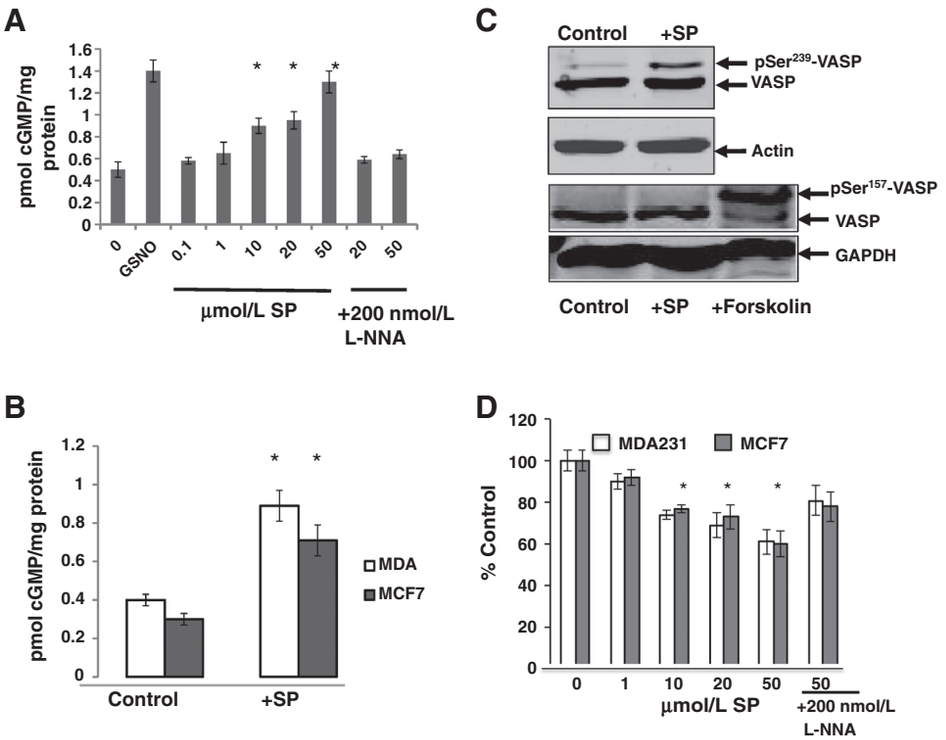

Figure 1.
Sepiapterin (SP) treatment *in vitro* and *in vivo* increases cGMP levels and PKG activity while reducing O_2^- formation. A, MCF7 cells were incubated with sepiapterin for 6 hours with or without 200 nmol/L of L-NNA. *, $P < 0.05$; $n = 3$. B, MCF7 and MDA-231 xenografts with or without 40 µg/mL sepiapterin in the drinking water. *, $P < 0.01$; $n = 4$. C, 24 hours after transfection with VASP, MCF7 cells were treated for 6 hours with 50 µmol/L of sepiapterin before harvesting and Western blot analysis for $pSer^{239}$ (top two panels) and $pSer^{157}$ (bottom two panels). As a positive control for PKA ($pSer^{157}$-VASP, cells were incubated with 10 µmol/L of forskolin. D, cells were treated with sepiapterin for 6 hours with or without 200 nmol/L of L-NNA. Cells were subsequently incubated with 10 µmol/L of dihydroethidium bromide for 30 minutes prior to analysis by HPLC. *, $P < 0.05$; $n = 3$.

that specifically measures its production from its oxidation of dihydroethidium to 2-hydroxyethidium (22). In both MCF7 and MDA-231 cells, sepiapterin treatment partially decreased O_2^- generation by a mechanism inhibited by L-NNA (Fig. 1D). These results, combined with the cGMP measurements, are consistent with sepiapterin recoupling of NOS activity.

Some investigations demonstrate that BH4 stabilizes a NOS dimer to SDS gel electrophoresis and is essential for a coupled catalysis (15, 29). We were unable to demonstrate this monomer–dimer transition with either iNOS or eNOS isoforms in sepiapterin-treated MCF7 cells with or without transfection to overexpress the NOS isoforms. Other studies have also not shown this monomer–dimer transition with BH4-dependent recoupling of NOS activity (30, 31). It is possible that BH4 stabilizes a specific conformation of the dimer that is unstable in SDS but necessary for NO synthesis (30).

Recoupling NOS downregulates β-catenin expression

Reduced β-catenin expression is observed with PKG overexpression in cultured colorectal tumor cells (13, 32) and in both colorectal and breast tumor cells by incubating with a cGMP phosphodiesterase inhibitor (33, 34). MCF7 cells were treated with 20 µmol/L sepiapterin with or without the PKG inhibitor KT5823 (a specific PKG inhibitor, IC_{50} 20 nmol/L), for up to 3 days. Cells were harvested each day and analyzed for β-catenin expression. Sepiapterin treatment *in vitro* for 72 hours reduced β-catenin expression by more than 60% via a mechanism inhibited by KT5823 (Fig. 2A and B). Almost complete ablation of β-catenin expression was observed in MCF7 xenografts from mice drinking water supplemented with sepiapterin for 48 hours (Fig. 2C). In spontaneous tumors from MMTVneu mice, inclusion of sepiapterin in their drinking water reduced β-catenin expression by 50% (Fig. 2D).

β-Catenin modulates tumor progression in part by interacting with the transcription factor TCF-4. We tested whether sepiapterin-induced downregulation of β-catenin resulted in a decreased TCF-4 promoter activity using a luciferase reporter construct (Fig. 2E). Luciferase activity was measured at 24 hours after transfection with cells treated with sepiapterin with or without KT5823 for the indicated times or after siRNA knockdown of PKG. Significant inhibition by 20 µmol/L sepiapterin was observed as early as 18 hours with maximal inhibition of 80% at 72 hours, the longest period tested. Sepiapterin inhibition of TCF-4 promoter activity was mostly reversed with KT5823. Treatment of cells for 24 hours with the cell-permeant cGMP analogue 8-Br-cGMP as a positive control reduced TCF-4 promoter activity by 80%. The pharmacologic inhibition of PKG activity and its effect on TCF-4 activity by sepiapterin was confirmed by siRNA knockdown of PKG expression.

Recoupling NOS inhibits NF-κB promoter activity

A key link between inflammation and oncogenesis is the transcription factor NF-κB. NF-κB is constitutively active in cancer cells due to autocrine and paracrine factors produced in the inflammatory microenvironment. NF-κB activity is both positively and negatively affected by ROS/RNS—nitration of Tyr^{181} of IκBα activates NF-κB (10), whereas S-nitrosylation of Cys^{38} of the p65 subunit inhibits (12). Treatment of MCF7 cells with 20 µmol/L sepiapterin completely eliminated basal Tyr nitration of IκBα (Fig. 3A). Figure 3B shows that increasing sepiapterin concentration augments levels of S-nitrosylated p65. A similar dose response was obtained when NF-κB promoter activity was measured in MCF7 cells transiently transfected with a luciferase based reporter construct. Incubation of these cells with sepiapterin reduced basal NF-κB promoter activity by 40% (Fig. 3C). A mutant $Cys^{38}Ser$ p65, which renders NF-κB insensitive to

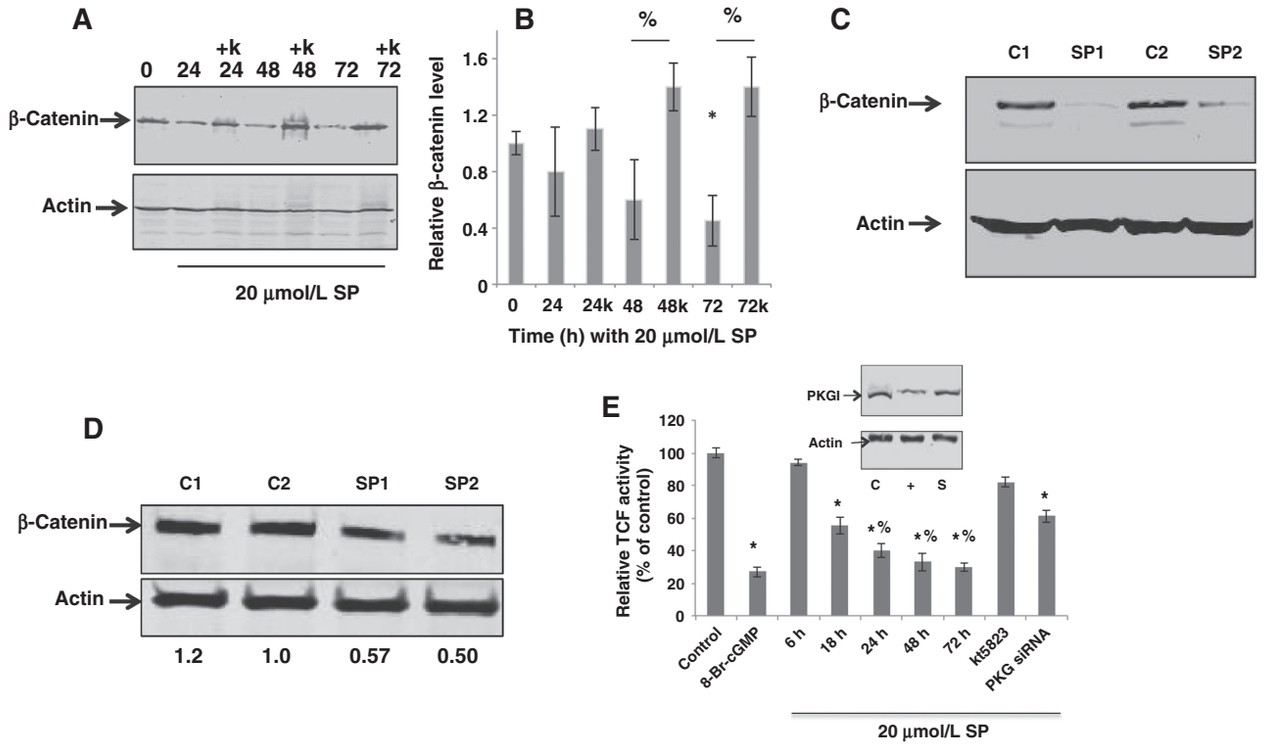

Figure 2.
Sepiapterin (SP) inhibits β-catenin expression and downstream signaling. A, MCF7 cells incubated with sepiapterin with or without the PKG inhibitor KT5823 (k), at 1 μmol/L. β-Catenin expression was analyzed by Western blot. B, densitometry of 3 experiments with β-catenin expression normalized to actin. *, relative to time zero; %, comparing with or without KT5823; $P < 0.05$, by two-way ANOVA. C, β-catenin levels relative to β-actin in MCF7 flank tumors with or without 40 μg/mL sepiapterin in their drinking water. C1 and C2, controls; SP1 and SP2, treated animals. D, β-catenin expression levels in tumors from MMTVneu mice with sepiapterin (mice SP1 and SP2) or without treatment (mice C1 and C2) for 4 days. E, TCF promoter activity measured with a luciferase reporter gene assay 24 hours after transfection. Phosphodiesterase-resistant 8-Br-cGMP (100 μmol/L) was used as a positive control. Inset: PKG1β expression in control (C) cells transfected with scrambled siRNA (S) or siRNA targeting PKG (+).

S-nitrosylation (12), was cotransfected with the luciferase reporter, and luciferase activity was measured with and without preincubation with sepiapterin. The reduction in NF-κB reporter activity obtained with sepiapterin was completely blocked by the overexpression of the mutant protein (Fig. 3C).

Sepiapterin treatment is cytotoxic to MCF7 and MDA-231 cells in tissue culture or as xenografts

A clonogenic assay *in vitro* and with xenografts establish that sepiapterin treatment at the concentrations used is cytotoxic to both MCF7 and MDA-231 breast carcinoma cells (Fig. 4A and B). We tested whether the cytotoxic activity of sepiapterin could be inhibited by the NOS inhibitor L-NNA, previously shown to inhibit NOS in MCF7 but without cytotoxic activity *in vitro* by itself (19, 35). The present results confirmed these results, but also demonstrated that L-NNA completely inhibited sepiapterin-induced cell killing (Fig. 4C). The PKG inhibitor KT5823 was equally ineffective as a cytotoxic agent but abrogated sepiapterin cytotoxicity.

Because L-NNA is cytotoxic to tumors *in vivo*, and because the sepiapterin reductase inhibitor NAS blocks the sepiapterin-induced increase in BH4:BH2 (Table 2), we tested whether inhibiting the BH4 salvage pathway with NAS blocks the sepiapterin cytotoxicity *in vivo*. Treatment of mice with NAS blocked tumor cell killing by sepiapterin, as measured by the *ex vivo* clonogenic assay of MCF7 xenograft tumors (Fig. 4D).

Sepiapterin is an antioxidant and shown to possibly protect sGC from oxidant inactivation (20). To rule out this role in the cytotoxic activity of sepiapterin, cells were incubated with, tetrahydroneopterin (NHP4), a biopterin with equivalent free radical scavenging activity as sepiapterin but unable to participate as a cofactor for NOS (20). As shown in Fig. 4C, NHP4 at concentrations equal to those used with sepiapterin was not cytotoxic.

The effects of prolonged sepiapterin treatment on tumor growth and animal survival were tested with MDA-231 xenografts. As shown in Supplementary Fig. S3 continuous oral supplementation over weeks provides a significant survival advantage. Future studies are required to determine how much this is due to sepiapterin effects on tumor cells and how much on supporting stromal cells.

Sepiapterin reduces tumor progression in the MMTVneu mouse assessed by FDG PET/CT and Ki67 staining

Antitumor activity of sepiapterin was also evaluated with a spontaneous cancer model, the MMTVneu mouse using FDG-PET/CT and Ki67 staining of tumors after animal sacrifice (Fig. 5). PET/CT scans before and after 5 days of oral sepiapterin (Fig. 5A) were quantified from 9 tumors (6 mice, 3 of

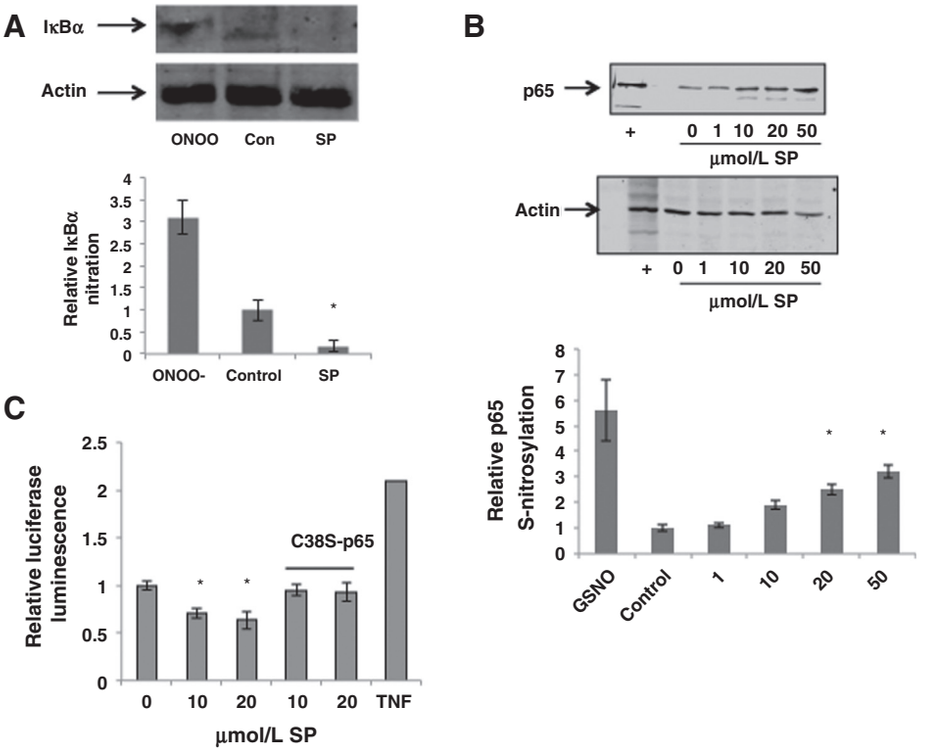

Figure 3.
Sepiapterin (SP) inhibits NF-κB transcriptional activity. A, MCF7 cells were incubated with or without 20 μmol/L sepiapterin for 6 hours, and lysates were immunopurified with anti-IκBα and probed for 3-nitrotyrosine. As a positive control, cell lysates were treated with $ONOO^-$. Results from 3 experiments were quantified by densitometry and are shown in the bar graph ($n = 3$, $P < 0.01$). B, MCF7 cells were incubated with sepiapterin for 6 hours before analysis of S-nitrosylation. GSNO (+) was added as a positive control. Total cell lysates were probed for actin as loading controls (bottom). $n = 3$; *, $P < 0.05$. C, the effect of 6 hours of sepiapterin on basal NF-κB promoter activity was determined with a luciferase-based reporter with tumor necrosis factor as a positive control. Some MCF7 cells were cotransfected with the NF-κB reporter plasmid and the p65 $Cys^{38}Ser$ mutant. Results represent the average of triplicate samples ($n = 3$; *, $P < 0.05$).

which carried 2 tumors) and analyzed for changes in FDG uptake (Fig. 5B). The percentage of decreases in FDG uptake by tumors varied significantly between animals and indeed between tumors from the same mouse (m001, m004, and m005). In all mice, except m005, sepiapterin reduced FDG uptake. When results from this mouse were censored in the

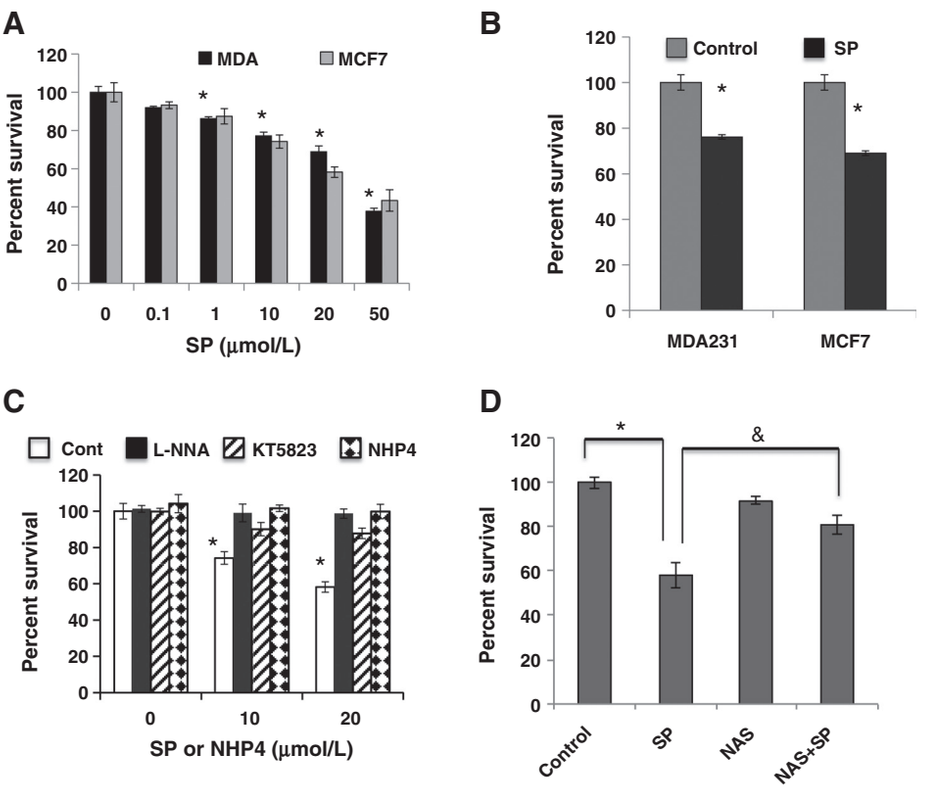

Figure 4.
Sepiapterin (SP) is cytotoxic to mammary carcinoma cells *in vitro* and in tumor xenografts. A, MCF7 and MDA-231 breast carcinoma cells *in vitro* were incubated with sepiapterin for 16 hours prior to plating for colony formation ($n = 3$; *, $P < 0.05$). B, for the *ex vivo* clonogenic assay of tumor xenografts, mice drank sepiapterin at 40 μg/mL for 48 hours before isolating single tumor cells for the clonogenic assay ($n = 3$; *, $P < 0.05$). C, *in vitro* clonogenic assays comparing the effects of NHP4 and sepiapterin (at the indicated concentrations) and the PKG inhibitor KT5823 (1 μmol/L) and NOS inhibitor L-NNA (200 nmol/L) on sepiapterin cytotoxicity ($n = 3$; *, $P < 0.05$). D, animals bearing MDA-231 flank xenografts with and without drinking sepiapterin-doped water and with or without the sepiapterin reductase inhibitor NAS delivered i.p. at 10 mg/kg the day before starting sepiapterin, on the day starting sepiapterin, and 24 hours later. Animals were sacrificed at 48 hours after sepiapterin treatment. $n = 3$; *, $P < 0.05$, comparing treated versus untreated, and $n = 3$; *, $P < 0.05$.

analysis, sepiapterin reduced FDG uptake by 25% ($P < 0.019$). When the data from this mouse were included in the analysis, FDG uptake was reduced by 21% ($P < 0.062$).

Reasons for this variability in FDG uptake are unclear. However, there were some tumors with tissue extracts available for BH4:BH2 analysis, including m005. A linear correlation ($P = 0.01$) was established between BH4:BH2 at the end of treatment and FDG uptake (Fig. 5C). BH4:BH2 of the two tumors of sepiapterin -treated m005 (1.1 and 1.3) were not significantly different from the average ratio for untreated MMTVneu tumors (1.0 ± 0.2; Table 1). Because we did not monitor water consumption separately for each mouse, it was possible that m005 did not consume enough sepiapterin to enhance the BH4:BH2. Other mechanisms, including poor tumor vascularization, are also possible. For the tumor with greatest reduction in FDG uptake (−72%, m004, tumor 6), BH4:BH2 was 3.9, similar to that observed for the normal mammary fat pad of the MMTVneu mouse (3.8 ± 0.5; Table 1).

Ki67 staining, a marker for actively proliferating cells, was used to confirm that sepiapterin reduced tumor growth (Fig. 5D). Representative immunofluorescence images of DAPI- and Ki67-stained sections of tumors from mice with and without sepiapterin treatment are shown along with a statistical evaluation from 5 randomly chosen tumor slices from three control and three treated animals. Sepiapterin treatment for 5 days reduced Ki67 staining by 60%.

Discussion

The major finding of this study is that regardless of tumor type and whether cells are cultured or derived from tumors, BH4:BH2 is significantly lower than normal tissues. Furthermore, BH4:BH2

A

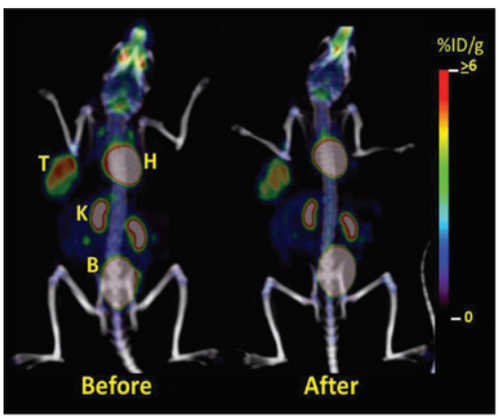

B

Mouse ID	Tumor number	Body wt. (g) pre SP	Body wt. (g) post SP	%ID/g pre SP	%ID/g post SP	% Change in FDG uptake
M001	T1	26.1	25.8	11.440	9.305	−18.7
M001	T2			10.990	7.447	−32.2
M002	T3	27.7	28.8	7.453	4.671	−37.3
M003	T4	26.1	28.7	5.785	5.175	−10.6
M004	T5	26.3	25.8	5.178	4.941	−4.6
M004	T6			6.353	1.782	−72.0
M005	T7	26.5	28.7	4.701	4.683	−0.4
M005	T8			5.499	7.343	+33.5
M006	T9	26.2	26.8	7.141	6.457	−9.6

Tumor samples	Pre-SP %ID/g ± STD	Post-SP %ID/g ± STD	Matched 2-tail *t* test
Total average ($n = 9$)	7.28 ± 2.50	5.76 ± 2.17	$P = 0.062$
Censored average ($n = 7$)	7.51 ± 2.48	5.66 ± 2.38	$P = 0.019$

C

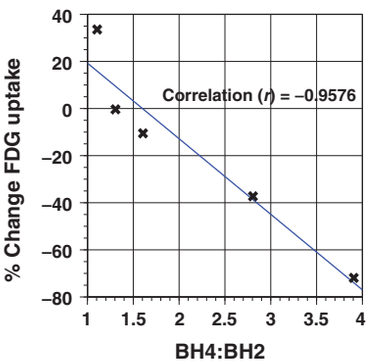

D

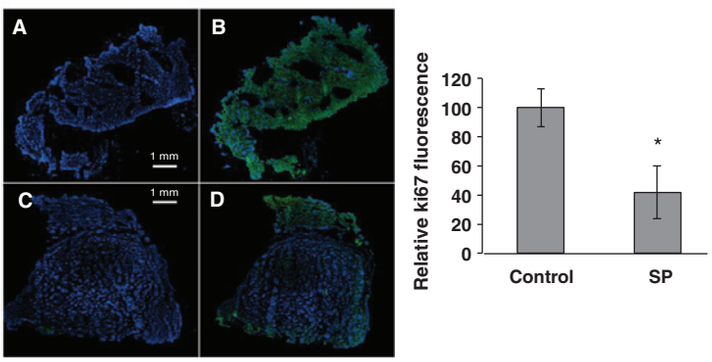

Figure 5.
PET-FDG and Ki67 IHC analyses of the effects of sepiapterin (SP) on MMTVneu tumor growth. A, PET/CT scans for mouse m003, tumor #4 (B) before and 5 days after starting sepiapterin treatment by inclusion of sepiapterin in its drinking water. T, tumor; H, heart; K, kidney; B, bladder. B, tabulated summary of results with 6 mice and 9 tumors (3 mice had 2 tumors each). The before and after results were analyzed by a matched two-tailed *t* test for all 9 tumors and also with the results from animal m005 censored. C, percentage of change in FDG uptake plotted against the BH4:BH2 for those tumors for which biopterin measurements were made: tumors #3, #4, #6, #7, and #8. The Pearson product moment correlation calculation determined the linear correlation between BH4:BH2 and FDG uptake. D, all Images were tissue slices stained with DAPI and a fluorophore secondary antibody. Images A and B are from adjacent slices of a tumor from non–sepiapterin-treated mouse. Images C and D are adjacent slices of a tumor from a mouse treated with sepiapterin for 5 days. Images B and D were incubated with a primary antibody against Ki67. The adjacent bar figure tabulates the results from tumors of 3 control animals and 3 sepiapterin-treated animals. Five pairs of random slices from each tumor were analyzed, and Ki67 image intensity was normalized with respect to DAPI staining. The statistical analysis was an unpaired Student *t* test with a $P < 0.01$ for control ($n = 15$) and for sepiapterin-treated animals ($n = 15$).

is enhanced by supplementing the culture medium or animal drinking water with a salvage pathway precursor, sepiapterin. Therapeutically, increasing BH4:BH2 caused tumor cell death in tissue culture or tumor xenografts, as defined by clonogenic survival and in spontaneous tumors by FDG-PET imaging and Ki67 staining.

Amino acid hydroxylases also use BH4 as a cofactor. Previous investigations suggest a growth-promoting, antiapoptotic role for serotonin, a product of tryptophan hydroxylase activity (36). This is contrary to the growth-inhibitory properties observed with sepiapterin *in vitro*, implying that any increase in tryptophan hydroxylase activity due to an increased BH4:BH2 is of lesser importance in effecting tumor growth. Future studies may need to consider both pro- and antiangiogenic activities of serotonin (37, 38).

Low levels of cGMP due to enhanced expression of PDE5, a cGMP-specific phosphodiesterase, characterize some cancer cells (14). Increasing cGMP levels by inhibiting PDE5 blocks MDA-231 and ZR75-1 breast cancer cell growth but not growth of nontransformed human mammary epithelial cells that do not express PDE5 (14, 34). Although not all downstream targets of cGMP/PKG are known, inhibition of PDE5 is associated with downregulation of β-catenin expression and downstream TCF-4 promoter activity in these breast cancer cell lines (14, 34). Our findings demonstrate that increased cellular cGMP levels and PKG activity, reduced β-catenin expression and TCF-4 promoter activity, and enhanced tumor cell killing are also obtained by modulating BH4:BH2 with a natural endogenous molecule.

The effects of NOS recoupling on tumor cell viability cannot be completely explained by enhanced PKG activity. This is clearly seen in the experiments demonstrating that increasing BH4:BH2 results in decreased tyrosine nitration of IκBα but increased S-nitrosylation of the p65 subunit of NF-κB partially inhibiting the latter's transcriptional activity (Fig. 3). Other regulatory proteins potentially involved in tumor growth are also posttranslationally modified by either Tyr nitration, e.g., PP2A, p53 (10, 11, 35), or Cys S-nitrosylation or oxidation, e.g., protein Tyr phosphatases, ras (6, 7).

Several mechanisms potentially contribute to the decreased BH4:BH2 of cancer cells. Overexpression of the rate-limiting enzyme for BH4 synthesis GCH1 significantly increases the BH4:BH2 in MCF7 cells, suggesting that either reduced GCH1 expression or activity may have a role. Some studies indicate that proteasomal degradation of GCH1 is a key regulatory factor in BH4 synthesis and it is thought to be one mechanism for the BH4 deficiency in diabetes mellitus (39). Proteasomal degradation of GCH1 is blocked by metformin-induced AMPK activation, resulting in the recoupling of eNOS in endothelial cells (40, 41). On the other hand, a recent report indicates that in some tumors GCH1 expression might actually be increased (42). This study did not, however, evaluate functional consequence such as BH4:BH2 or cGMP. GCH1 activity is also regulated by an inhibitory protein, GCH1 feedback regulatory protein (GFRP). GFRP inhibits GCH1 by a direct binding mechanism that requires BH4 at the interface between the two proteins (43).

DFHR and dihydropteridine reductase (DHPR), acting together or individually, can by salvage synthesize BH4. It is unlikely, given the DNA synthesis requirements of cancer cells that reduced DHFR activity account for reduced BH4. DHPR reduces quinonoid dihydrobiopterin, an intermediate in the peroxynitrite oxidation of BH4 to BH2, back to BH4. There are reports that expression levels of DHPR are reduced in conditions where BH4:BH2 is low, e.g., diabetes (44). A genetic disorder of reduced DHPR is treated with BH4 (45). Early investigations also indicate that DHPR activities are lower in solid tumor tissue relative to their normal tissue counterpart (46).

Results in Table 2 demonstrate potential mechanisms by which NOS produced peroxynitrite that oxidizes BH4, further propagating uncoupling (47). A related mechanism follows from the cellular proximity relationships between NOS and O_2^- generating activities. Both eNOS and iNOS, the major NOS isoforms in epithelial tumor cells, reside at least in part at the plasma membrane. eNOS has a complicated relationship to the plasma membrane being targeted to plasma membrane caveolae through a mechanism involving N-myristoylation and palmitoylation and forming a complex with caveolin-1 (48). Binding to caveolin-1 induces an inhibitory conformation of eNOS that is relieved upon Akt phosphorylation of eNOS. This positioning of eNOS at caveolae puts it in close proximity to the O_2^- generating NADPH oxidases, potentially generating peroxynitrite that rapidly reacts with BH4, thereby initiating uncoupling (49). GCH1 has also been localized to caveolae in some cells (50). Results in Table 2 demonstrate that NADPH oxidase is also a potential contributor in the oxidation of BH4.

NOS uncoupling can occur under other conditions, e.g., low [Arg], or elevated levels of endogenous NOS inhibitors (17, 18). Regardless of the mechanism, NOS uncoupling represents a critical switching mechanism for tumor cell growth. When the primary product of NOS is NO, downstream signaling is dominated by NO-dependent pathways (e.g., sGC/PKG and S-nitrosylation). Uncoupled NOS, on the other hand, produces oxidants such as peroxynitrite and O_2^-, initiating different downstream signaling that for tumor cells are proproliferative and antiapoptotic, e.g., NF-κB. The focus of this study has been on the tumor cell. Given the chronic inflammatory conditions of solid tumors, it is likely that stromal cells also exhibit uncoupled NOS activity and, by this mechanism, are subverted to support tumor growth. Our results also suggest a novel anticancer therapy that by its mode of action should have minimal normal tissue toxicity. Synthetic BH4 (Kuvan) is presently being using to treat certain forms of phenylketonuria and is being tested in clinical trials to reduce endothelial dysfunction.

Disclosure of Potential Conflicts of Interest

G. Sundaresan reports receiving speakers bureau honoraria from the University of Virginia. No potential conflicts of interest were disclosed by the other authors.

Authors' Contributions

Conception and design: C.S. Rabender, R.J. Cardnell, J. Zweit, R.B. Mikkelsen
Development of methodology: C.S. Rabender, G. Sundaresan, V.A. Yakovlev, J. Zweit
Acquisition of data (provided animals, acquired and managed patients, provided facilities, etc.): C.S. Rabender, A. Alam, G. Sundaresan, R.J. Cardnell, V.A. Yakovlev, J. Zweit, P.R. Graves, R.B. Mikkelsen
Analysis and interpretation of data (e.g., statistical analysis, biostatistics, computational analysis): C.S. Rabender, A. Alam, G. Sundaresan, N.D. Mukhopadhyay, J. Zweit, P.R. Graves, R.B. Mikkelsen
Writing, review, and/or revision of the manuscript: C.S. Rabender, A. Alam, G. Sundaresan, R.J. Cardnell, V.A. Yakovlev, N.D. Mukhopadhyay, J. Zweit, R.B. Mikkelsen
Administrative, technical, or material support (i.e., reporting or organizing data, constructing databases): C.S. Rabender, G. Sundaresan, J. Zweit
Study supervision: C.S. Rabender, G. Sundaresan, V.A. Yakovlev, J. Zweit, R.B. Mikkelsen

Acknowledgments

The authors thank Dr. Catherine Dumur and Ms. Pamela Grizzard of the Massey Cancer Center Tissue Acquisition Core for providing the human tissue samples.

Grant Support

This work was supported by NIH grants 5R01CA090881 (R.B. Mikkelsen) and T32CA113277 (C.S. Rabender and R.J. Cardnell). Additional funding for Tissue Acquisition Core and a pilot project came from the Massey Cancer Center grant 5P30CA016059-33.

The costs of publication of this article were defrayed in part by the payment of page charges. This article must therefore be hereby marked *advertisement* in accordance with 18 U.S.C. Section 1734 solely to indicate this fact.

Received February 13, 2015; accepted February 21, 2015; published OnlineFirst February 27, 2015.

References

1. Balkwill F, Mantovani A. Inflammation and cancer: back to Virchow? Lancet 2001;357:539–45.
2. Thomas DD, Ridnour LA, Isenberg JS, Flores-Santana W, Switzer CH, Donzelli S, et al. The chemical biology of nitric oxide: implications in cellular signaling. Free Radic Biol Med 2008;45:18–31.
3. Cardnell RJ, Mikkelsen RB. Nitric oxide synthase inhibition enhances the antitumor effect of radiation in the treatment of squamous carcinoma xenografts. PLoS One 2011;6:e20147.
4. Tozer GM, Prise VE, Chaplin DJ. Inhibition of nitric oxide synthase induces a selective reduction in tumor blood flow that is reversible with L-arginine. Cancer Res 1997;57:948–55.
5. Du Q, Zhang X, Liu Q, Bartels CE, Geller DA. Nitric oxide production upregulates Wnt/beta-catenin signaling by inhibiting Dickkopf-1. Cancer Res 2013;73:6526–37.
6. Lim KH, Ancrile BB, Kashatus DF, Counter CM. Tumour maintenance is mediated by eNOS. Nature 2008;452:646–9.
7. Barrett DM, Black SM, Todor H, Schmidt-Ullrich RK, Dawson KS, Mikkelsen RB. Inhibition of protein-tyrosine phosphatases by mild oxidative stresses is dependent on S-nitrosylation. J Biol Chem 2005;280:14453–61.
8. Sturla LM, Amorino G, Alexander MS, Mikkelsen RB, Valerie K, Schmidt-Ullrichr RK. Requirement of Tyr-992 and Tyr-1173 in phosphorylation of the epidermal growth factor receptor by ionizing radiation and modulation by SHP2. J Biol Chem 2005;280:14597–604.
9. Delgado-Esteban M, Martin-Zanca D, Andres-Martin L, Almeida A, Bolanos JP. Inhibition of PTEN by peroxynitrite activates the phosphoinositide-3-kinase/Akt neuroprotective signaling pathway. J Neurochem 2007;102:194–205.
10. Yakovlev VA, Barani IJ, Rabender CS, Black SM, Leach JK, Graves PR, et al. Tyrosine nitration of IkappaBalpha: a novel mechanism for NF-kappaB activation. Biochemistry 2007;46:11671–83.
11. Yakovlev VA. Nitric oxide-dependent downregulation of BRCA1 expression promotes genetic instability. Cancer Res 2013;73:706–15.
12. Marshall HE, Hess DT, Stamler JS. S-nitrosylation: physiological regulation of NF-kappaB. Proc Natl Acad Sci U S A 2004;101:8841–2.
13. Browning DD, Kwon IK, Wang R. cGMP-dependent protein kinases as potential targets for colon cancer prevention and treatment. Future Med Chem 2010;2:65–80.
14. Windham PF, Tinsley HN. cGMP signaling as a target for the prevention and treatment of breast cancer. Semin Cancer Biol 2015;31:106–10.
15. Cai S, Khoo J, Channon KM. Augmented BH4 by gene transfer restores nitric oxide synthase function in hyperglycemic human endothelial cells. Cardiovasc Res 2005;65:823–31.
16. Luiking YC, Ten Have GA, Wolfe RR, Deutz NE. Arginine de novo and nitric oxide production in disease states. Am J Physiol Endocrinol Metab 2012;303:E1177–89.
17. Alkaitis MS, Crabtree MJ. Recoupling the cardiac nitric oxide synthases: tetrahydrobiopterin synthesis and recycling. Curr Heart Fail Rep 2012;9:200–10.
18. Zweier JL, Chen CA, Druhan LJ. S-glutathionylation reshapes our understanding of endothelial nitric oxide synthase uncoupling and nitric oxide/reactive oxygen species-mediated signaling. Antioxid Redox Signal 2011;14:1769–75.
19. Cardnell RJ, Rabender CS, Ross GR, Guo C, Howlett EL, Alam A, et al. Sepiapterin ameliorates chemically induced murine colitis and azoxymethane-induced colon cancer. J Pharmacol Exp Ther 2013;347:117–25.
20. Schmidt K, Neubauer A, Kolesnik B, Stasch JP, Werner ER, Gorren AC, et al. Tetrahydrobiopterin protects soluble guanylate cyclase against oxidative inactivation. Mol Pharmacol 2012;82:420–7.
21. Shimazu T, Otani H, Yoshioka K, Fujita M, Okazaki T, Iwasaka T. Sepiapterin enhances angiogenesis and functional recovery in mice after myocardial infarction. Am J Physiol Heart Circ Physiol 2011;301:H2061–72.
22. Zielonka J, Vasquez-Vivar J, Kalyanaraman B. Detection of 2-hydroxyethidium in cellular systems: a unique marker product of superoxide and hydroethidine. Nat Protoc 2008;3:8–21.
23. Werner ER, Blau N, Thony B. Tetrahydrobiopterin: biochemistry and pathophysiology. Biochem J 2011;438:397–414.
24. Fallahian F, Karami-Tehrani F, Salami S, Aghaei M. Cyclic GMP induced apoptosis via protein kinase G in oestrogen receptor-positive and -negative breast cancer cell lines. Febs J 2011;278:3360–9.
25. Schwappacher R, Rangaswami H, Su-Yuo J, Hassad A, Spitler R, Casteel DE. cGMP-dependent protein kinase Ibeta regulates breast cancer cell migration and invasion via interaction with the actin/myosin-associated protein caldesmon. J Cell Sci 2013;126:1626–36.
26. Reif DW, McCreedy SA. N-nitro-L-arginine and N-monomethyl-L-arginine exhibit a different pattern of inactivation toward the three nitric oxide synthases. Arch Biochem Biophys 1995;320:170–6.
27. Abdelmagid SA, Rickard JA, McDonald WJ, Thomas LN, Too CK. CAT-1-mediated arginine uptake and regulation of nitric oxide synthases for the survival of human breast cancer cell lines. J Cell Biochem 2011;112:1084–92.
28. Garvey EP, Oplinger JA, Furfine ES, Kiff RJ, Laszlo F, Whittle BJ, et al. 1400W is a slow, tight binding, and highly selective inhibitor of inducible nitric-oxide synthase in vitro and in vivo. J Biol Chem 1997;272:4959–63.
29. Benson MA, Batchelor H, Chuaiphichai S, Bailey J, Zhu H, Stuehr DJ, et al. A pivotal role for tryptophan 447 in enzymatic coupling of human endothelial nitric oxide synthase (eNOS): effects on tetrahydrobiopterin-dependent catalysis and eNOS dimerization. J Biol Chem 2013;288:29836–45.
30. Rodriguez-Crespo I, Gerber NC, Ortiz de Montellano PR. Endothelial nitric-oxide synthase. Expression in Escherichia coli, spectroscopic characterization, and role of tetrahydrobiopterin in dimer formation. J Biol Chem 1996;271:11462–7.
31. Whitsett J, Martasek P, Zhao H, Schauer DW, Hatakeyama K, Kalyanaraman B, et al. Endothelial cell superoxide anion radical generation is not dependent on endothelial nitric oxide synthase-serine 1179 phosphorylation and endothelial nitric oxide synthase dimer/monomer distribution. Free Radic Biol Med 2006;40:2056–68.
32. Kwon IK, Wang R, Thangaraju M, Shuang H, Liu K, Dashwood R, et al. PKG inhibits TCF signaling in colon cancer cells by blocking beta-catenin expression and activating FOXO4. Oncogene 2010;29:3423–34.
33. Li N, Xi Y, Tinsley HN, Gurpinar E, Gary BD, Zhu B, et al. Sulindac selectively inhibits colon tumor cell growth by activating the cGMP/PKG pathway to suppress Wnt/beta-Catenin signaling. Mol Cancer Ther 2013;12:1848–59.
34. Tinsley HN, Gary BD, Keeton AB, Lu W, Li Y, Piazza GA. Inhibition of PDE5 by sulindac sulfide selectively induces apoptosis and attenuates oncogenic Wnt/beta-catenin-mediated transcription in human breast tumor cells. Cancer Prev Res 2011;4:1275–84.
35. Yakovlev VA, Bayden AS, Graves PR, Kellogg GE, Mikkelsen RB. Nitration of the tumor suppressor protein p53 at tyrosine 327 Promotes p53 oligomerization and activation. Biochemistry 2010;49:5331–9.
36. Pai VP, Marshall AM, Hernandez LL, Buckley AR, Horseman ND. Altered serotonin physiology in human breast cancers favors paradoxical growth and cell survival. Breast Cancer Res 2009;11:R81.
37. Nocito A, Dahm F, Jochum W, Jang JH, Georgiev P, Bader M, et al. Serotonin regulates macrophage-mediated angiogenesis in a mouse model of colon cancer allografts. Cancer Res 2008;68:5152–8.

38. Qin L, Zhao D, Xu J, Ren X, Terwilliger EF, Parangi S, et al. The vascular permeabilizing factors histamine and serotonin induce angiogenesis through TR3/Nur77 and subsequently truncate it through thrombospondin-1. Blood 2013;121:2154–64.
39. Sharma S, Sun X, Kumar S, Rafikov R, Aramburo A, Kalkan G, et al. Preserving mitochondrial function prevents the proteasomal degradation of GTP cyclohydrolase I. Free Radic Biol Med 2012;53:216–29.
40. Wang S, Xu J, Song P, Viollet B, Zou MH. In vivo activation of AMP-activated protein kinase attenuates diabetes-enhanced degradation of GTP cyclohydrolase I. Diabetes 2009;58:1893–901.
41. Kim YH, Hwang JH, Kim KS, Noh JR, Gang GT, Oh WK, et al. Enhanced activation of NAD(P)H: quinone oxidoreductase 1 attenuates spontaneous hypertension by improvement of endothelial nitric oxide synthase coupling via tumor suppressor kinase liver kinase B1/adenosine 5′-monophosphate-activated protein kinase-mediated guanosine 5′-triphosphate cyclohydrolase 1 preservation. J Hypertens 2014;32:306–17.
42. Pickert G, Lim HY, Weigert A, Haussler A, Myrczek T, Waldner M, et al. Inhibition of GTP cyclohydrolase attenuates tumor growth by reducing angiogenesis and M2-like polarization of tumor associated macrophages. Int J Cancer 2013;132:591–604.
43. Li L, Rezvan A, Salerno JC, Husain A, Kwon K, Jo H, et al. GTP cyclohydrolase I phosphorylation and interaction with GTP cyclohydrolase feedback regulatory protein provide novel regulation of endothelial tetrahydrobiopterin and nitric oxide. Circ Res 2010;106:328–36.
44. Lee CK, Han JS, Won KJ, Jung SH, Park HJ, Lee HM, et al. Diminished expression of dihydropteridine reductase is a potent biomarker for hypertensive vessels. Proteomics 2009;9:4851–8.
45. Coughlin CR 2nd, Hyland K, Randall R, Ficicioglu C. Dihydropteridine reductase deficiency and treatment with tetrahydrobiopterin: a case report. JIMD Rep 2013;10:53–6.
46. Sanchez-Urretia L, Pierce CE, Greengard O. Dihydropteridine reductase activity of adult, fetal and neoplastic tissues. Enzyme 1978;23:346–52.
47. Kuzkaya N, Weissmann N, Harrison DG, Dikalov S. Interactions of peroxynitrite, tetrahydrobiopterin, ascorbic acid, and thiols: implications for uncoupling endothelial nitric-oxide synthase. J Biol Chem 2003;278:22546–54.
48. Goligorsky MS, Li H, Brodsky S, Chen J. Relationships between caveolae and eNOS: everything in proximity and the proximity of everything. Am J Physiol Renal Physiol 2002;283:F1–10.
49. Reilly SN, Jayaram R, Nahar K, Antoniades C, Verheule S, Channon KM, et al. Atrial sources of reactive oxygen species vary with the duration and substrate of atrial fibrillation: implications for the antiarrhythmic effect of statins. Circulation 2011;124:1107–17.
50. Peterson TE, d'Uscio LV, Cao S, Wang XL, Katusic ZS. Guanosine triphosphate cyclohydrolase I expression and enzymatic activity are present in caveolae of endothelial cells. Hypertension 2009;53:189–95.